Can the Transition from Tunneling to Hopping in Molecular Junctions Be Predicted by Theoretical Calculation?

HONGMEI LIU,[1,2] ZHENZHEN ZHAO,[1] NAN WANG,[1] CUI YU,[1] JIANWEI ZHAO[1]
[1]*Key laboratory of Analytical Chemistry for Life Science (Ministry of Education), School of Chemistry and Chemical Engineering, Nanjing University, Nanjing 210008, People's Republic of China*
[2]*Experimental Center, Linyi University, Shuangling Road, Linyi 276000, People's Republic of China*

Received 17 November 2010; Revised 14 December 2010; Accepted 17 December 2010
DOI 10.1002/jcc.21749
Published online 1 March 2011 in Wiley Online Library (wileyonlinelibrary.com).

Abstract: The electron transport mechanism changes from tunneling to hopping as molecular length increases. To validate the theoretical simulation after the transition point and clarify influence of electronic structures on the transition, we calculated the conductance of a series of conjugated molecules by density functional theory together with the nonequilibrium Green's function. We found that the highest occupied molecular orbital energy level, transmission spectrum, and the reorganization energy are good indicators for the transition of the electron transport mechanism. The calculated resistances of short junctions (<50 Å, before the transition point) are consistent with the experimental result, following the tunneling mechanism. However, the theoretical predication failed for long molecules, indicating the limitation of the theoretical framework of elastic scattering when the electron transport mechanism changes to hopping.

 J Comput Chem 32: 1687–1693, 2011

Key words: molecular junction; theoretical simulation; electron tunneling; electron hopping; reorganization energy

Introduction

Recently, the electron transport mechanisms across a single molecule have been experimentally investigated in some detail.[1,2] To directly measure the current-voltage characteristic of a metal-molecule-metal junction, a number of experimental methods have been developed, such as conducting probe atomic force microscopy (CP-AFM),[3] scanning tunneling microscopy (STM),[4] and mechanical break junctions.[5] On the basis of experimental results, a variety of electron transport mechanisms have been proposed, depending on molecular size and structure, as well as temperature.

As predicted theoretically, and indicated by many experiments, coherent tunneling predominates in electron transport of short donor-bridge-acceptor systems.[1,6–8] The tunneling (Fig. 1a) is based on the probability of electrons traversing a barrier with a certain thickness and height and maintains the phase of the electron. In other words, there is a finite probability of finding the electron on the other side of the barrier, without requiring nuclear motion.[1] The tunneling current at low bias can be simply depicted by the Simmons relation.[9] The molecular resistance varies exponentially with length as depicted by eq (1),

$$R = R_0 \exp(\beta d) \tag{1}$$

where R_0 is the contact resistance, d is molecular length, and β is the tunneling attenuation factor.

In long molecular wires, electron transport can be dominated by the hopping mechanism (see Fig. 1a), which follows a classical Arrhenius relation [eq (2)],

$$k_{ET} = k_{ET}^{\circ} \exp(-E_a/kT) \tag{2}$$

where k_{ET} is the electron transport rate, E_a is an activation barrier, and k is the Boltzman constant. As hopping involves a

Correspondence to: J. Zhao. e-mail: zhaojw@nju.edu.cn.

Contract/grant sponsor: National Natural Science Foundation of China (NSFC); contract/grant numbers: 20821063, 20873063, 51071084

Contract/grant sponsor: National Basic Research Program of China (973 Program); contract/grant numbers: 2007CB936302, 2010CB732400

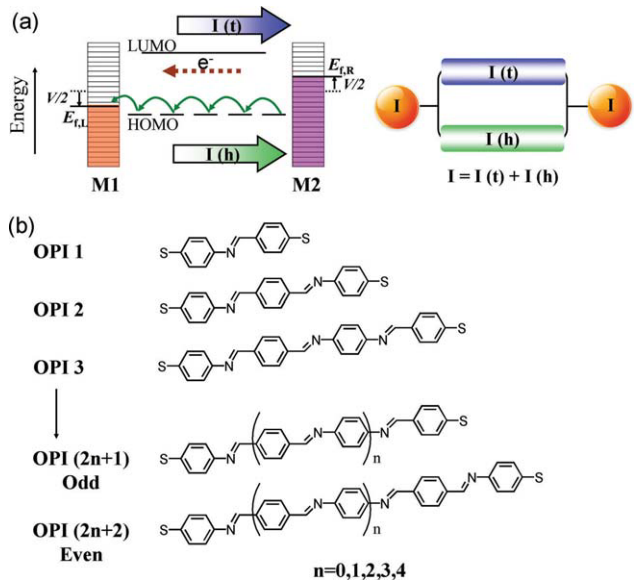

Figure 1. (a) Schematic energy level diagrams for tunneling and hopping. M1 and M2 denote the metallic electrodes. The Fermi level of M2 increases $V/2$ eV when junction bias is applied, whereas M1 changes oppositely. $I(t)$ is the current contributed by single-step tunneling and $I(h)$ corresponds the current of multistep hopping. (b) The chemical structures of OPI molecules.

series of transfers between the adjacent relatively stable sites, it does not exhibit the exponential distance dependence of current, but instead varies as $\sim d^{-1}$.[1,10]

A direct observation of the electron transport mechanism from tunneling to hopping was made by Choi et al.,[11–13] when they measured the resistance of a series of conjugated molecular wires. For short molecules, the length dependence is exponential, corresponding to the tunneling regime, and for long bridges, the resistance increases linearly because of the hopping mechanism adopted. A similar result was also found for oligo (*p*-phenylene ethynylene)s by Lu et al.[14] and other long conjugated molecular wires by Tao et al.[15] using STM break junction method. Tunneling and hopping are generally considered to be alternative electron transport mechanisms in molecular systems. However, as studied by Lambert et al.,[16] tunneling and hopping mechanisms are not mutually exclusive; indeed, it has been shown that both may be present within one system.[16] In this case, the total current of the molecular junction is composed of the tunneling and hopping components as shown in Figure 1(a).

Besides experimental measurements, the molecular conductance has also been calculated by theoretical simulations. The elastic scattering theory depicts the tunneling transport, which can be dealt with the nonequilibrium Green's function (NEGF)[17] combined with the density functional theory (DFT). Recently, NEGF-DFT method has been widely used to model quantum transport of atomic and molecular scale nanoelectronic devices under external electric field.[18,19] Although molecular length is short, the simulation provided reliable results.[20–23] However, it is not clear yet when the electron transport mechanism changes in a homologous series of molecules, and whether this technique treats hopping properly. On the other hand, molecular length is just a direct evidence of geometric structure for mechanism transition, how the electronic properties of the molecule influence the transition from the tunneling regime to the charge hopping regime? Therefore, this study will clarify the intrinsic factors relevant to the hopping mechanism.

Methodology

To gain insight into the reliability of the theoretical technique, we calculated the conductance of oligophenyleneimine (OPI) molecular junctions, because the conductivity has been exactly characterized experimentally by CP-AFM method.[11] The molecular wires vary from 12.9 to 71.7 Å as shown in Figure 1b. The calculation was performed by the Atomistic Toolkit 2.0 program[24–27] with NEGF-DFT method. Each OPI molecule was connected with Au(111) electrodes through two thiol groups forming Au-molecule-Au junction. Two hydrogen atoms were removed from the thiol groups as adsorption takes place and the adsorption site to the sulfur atom is a threefold hollow site of the Au plane. Then the full structure optimization of the molecules was performed by relaxing all atoms within a force tolerance of 0.1 eV/Å. The optimized molecule-electrode contact distance (S-Au distance) was in the range of 2.04–2.06 Å for all the molecules. We used the local density approximation with a

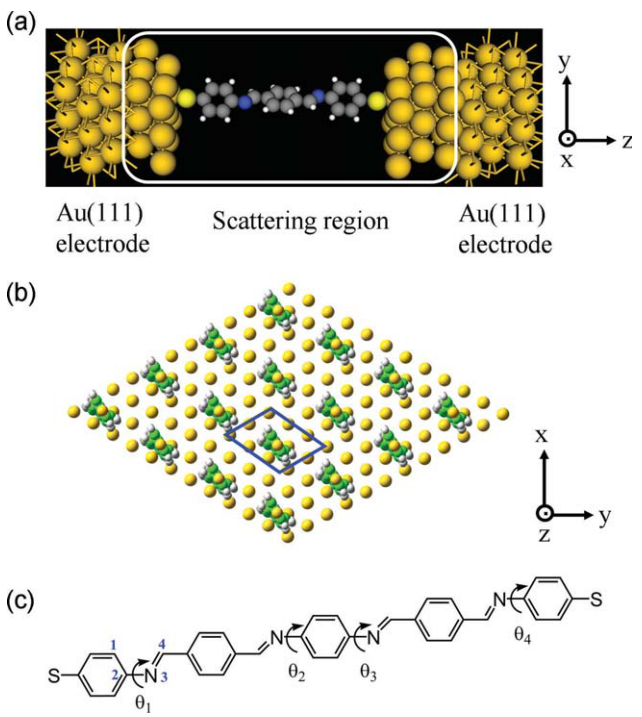

Figure 2. (a) Schematic illustration of a simplified model of the Au-molecule-Au junction for the conductance calculation. (b) Top view of the junction structure with periodic boundary conditions (the contour indicates the unit cell), taking OPI 4 for example. (c) Example for torsion angles of OPI molecules where OPI 4 is shown for reference.

Table 1. Torsion Angles for the OPI Molecules Optimized by the ATK Program with DZP Basis Set.

Molecules	Length (Å)	θ_1	θ_2	θ_3	θ_4	θ_5	θ_6	θ_7	θ_8	θ_9	θ_{10}
OPI 1	12.9	−32.1									
OPI 2	19.5	−30.5	31.2								
OPI 3	26.0	−31.3	27.2	−31.1							
OPI 4	32.5	−30.7	29.5	−28.7	31.2						
OPI 5	39.1	−31.0	28.8	−29.6	27.3	−31.1					
OPI 6	45.6	−31.4	28.4	−29.3	29.3	−27.9	31.5				
OPI 7	52.1	−31.5	28.8	−30.0	29.6	−29.9	28.2	−30.7			
OPI 8	58.7	−31.2	29.0	−29.2	29.1	−29.0	29.2	−28.9	31.6		
OPI 9	65.2	−31.3	28.9	−30.0	28.1	−30.0	28.3	−29.9	27.5	−30.9	
OPI 10	71.7	−31.2	29.0	−29.4	29.0	−29.1	29.1	−28.8	29.6	−28.7	31.7

All torsion angles are in degree (°) and θ_1 is the dihedral angle of C1—C2—N3—C4. Molecular length was determined as distance between two sulfur atoms, that is, the length of S-Molecule-S.

double-ζ plus polarization basis set for the molecules and single-ζ plus polarization basis set for the Au electrodes.

The general system for which transport calculations were performed consists of three parts: a left electrode, a scattering region, and a right electrode. The semi-infinite electrodes were modeled by two Au(111)-(3 × 3) surfaces with periodic boundary conditions, and Figures 2a and 2b shows the theoretical model and several repeat units. A supercell consists of two layers of 18 gold atoms to the left and three layers of 27 gold atoms to the right of the scattering region, where the difference in two sides is necessary to maintain the periodicity of the system.[28] It is reported that taking two layers of Au in the self-consistent cycle is enough to mitigate the finite size effect.[29] This system has been previously used to illustrate the scattering region in the literature.[20,21,30] Then the conductance was computed within the Landauer-Büttiker formalism.[17,31] The conductance is given by $G = G_0T(E_F)$, where $G_0 = 2e^2/h$ (e is the electronic charge and h is Planck's constant) is the quantum conductance and $T(E_F)$ is the transmission function at the Fermi level E_F. We performed the conductance calculation using the NEGF-DFT theories to simulate the electric behavior of the molecule sandwiched between the Au electrodes, including a full self-consistent-field treatment of the metal-molecule-metal junction.

To find the correlation between electronic structures and electron transport mechanism, we also evaluated the molecular energy level, the transmission spectrum, and the reorganization energy, because the ability of wire to transport a charge depends crucially on the reorganization energy.[32] The reorganization energy involved in the charge transfer process was carried out with the GAUSSIAN 03 program.[33] The geometric structure optimization of neutral state was performed at the DFT level with the B3LYP/6-31G* basis set, and the unrestricted DFT method was adopted for ions. The definition of reorganization energy is in the results and discussion section.

Results and Discussion

The OPI molecules generally exhibit a twisted conformation mostly due to the nitrogen atom, as shown in Figure 2c for the example. The absolute values of torsion angles of C—N bonds in the wires are typically 27–32°. The torsion angles obtained by DZP basis set are several degree lower than that determined at the B3LYP/6-31G** level of theory by Frisbie et al., which are given in the Supplemental Materials of ref. [12]. The detailed data of molecular length and dihedral angle θ for OPI oligomers are listed in Table 1. As the interlaced conformation breaks the π-conjugation over the whole molecule, the torsion angle quantitatively reduces molecular conductance as demonstrated by Venkataraman et al.[34,35] As a result, the OPI molecule is less conductive than the oligo phenylene vinylene with planar structure at the same length.[22] On the other hand, as the conjugated structure has been broken into several segments, the electron hopping via each energy well along the molecular wire becomes favored for those long systems. The twisted structure also infers that the intermolecular π-stacking effect is weak that can be neglected in the following discussion.

The molecular resistance of OPI is analyzed as a function of molecular length by varying the number of repeat units. To confirm the theoretical result obtained by the NEGF-DFT methods, Figure 3a gives the logarithmic dependence of resistance on molecular length. We can observe that the calculated resistance increases exponentially with molecular length in the left region. The linear fit (from OPI 1 to 6) indicates an exponential relation between resistance and length, which can be well described by eq (1). Furthermore, the tunneling attenuation factor of 0.25 $Å^{-1}$ for short OPI wires is consistent with 0.30 $Å^{-1}$ obtained by CP-AFM measurement.[11] The exponential increase of resistance indicates a tunneling mechanism while the length of the molecular wire is shorter than 50 Å. Similar results have also been proven by many other systems.[20–23] Therefore, we can conclude that for short molecular wires, the theoretical simulation based on the elastic scattering mechanism is reasonable and reliable.

When the wire is longer than 50 Å, the resistance still increases rapidly in general as plotted by the dashed line in Figure 3a. As the resistance falls into the scale of GΩ (from 0.35 GΩ for OPI 6 to 54 GΩ for OPI 10), a significant feature observed is the fluctuation. For example, the resistance of OPI 9 is even lower than that of OPI 8. The theoretical prediction did not give any evidence of existing of the transition point in the resistance line as wire increases. On the contrary, the experimental

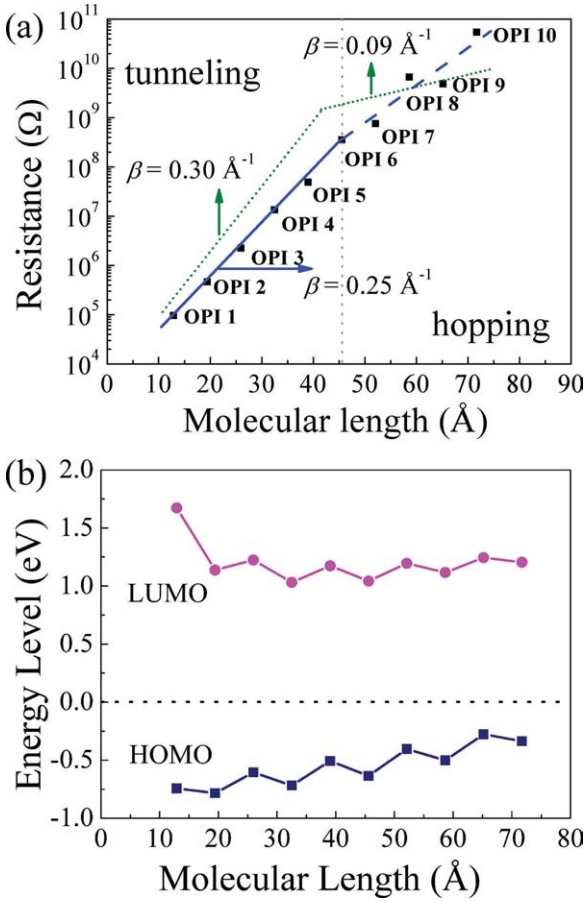

Figure 3. (a) Semilog plot of molecular resistance for OPI molecules obtained theoretically. Points show calculated data and the blue solid line is linear fit (OPI 1–6) yielding the β value of 0.25 $Å^{-1}$ from the slope. The correlation coefficient of the linear fit is 0.998. The vertical dotted line divides the figure into two parts, and the left and right regions correspond to the tunneling and hopping, respectively. The short dotted lines denote the experimental results with β = 0.30 and 0.09 $Å^{-1}$.[11] The molecular length is S-Molecule-S distance which is optimized by ATK. (b) The HOMO and LUMO energy levels of the OPI series.

results obtained by Choi et al.[11] clearly showed it when molecular length is 40 Å, indicating a change of electron transport mechanism from tunneling to hopping. For easy comparison, we also plotted the experimental data of the β value (0.09 $Å^{-1}$) in Figure 3a. The short dotted line indicates the attenuation of the transportation of the hopping mechanism. Additionally, we can observe that the OPI 6 belongs to the hopping region for the experimental result. As both tunneling and hopping mechanisms may be present within one system at the threshold,[8] the transition point just shows the change of dominant mechanism. For OPI 6, the charge hopping mainly contributes to the conductance, whereas the contribution of tunneling is small. However, only tunneling was considered in the theoretical calculation. Thus, the transition point measured by Choi et al.[11] appears before the calculated one.

Here, we note that the calculated resistance of single molecule is generally lower than the experimental result because of the approximation in the exchange-correlation functional.[36] The previous study has also confirmed that the resistance of 1,4-benzenediamine[37] obtained experimentally is six times larger than that obtained by NEGF-DFT.[38] For short OPI 1 model, the resistance of theoretical simulation is around 10^5 Ω slightly lower than the experimental one. However, for long conjugated molecular wires, the calculated resistance tends to be greater than the measured one. When the repeat unit number is 8, the dashed line crosses the short dotted line. The small resistance in

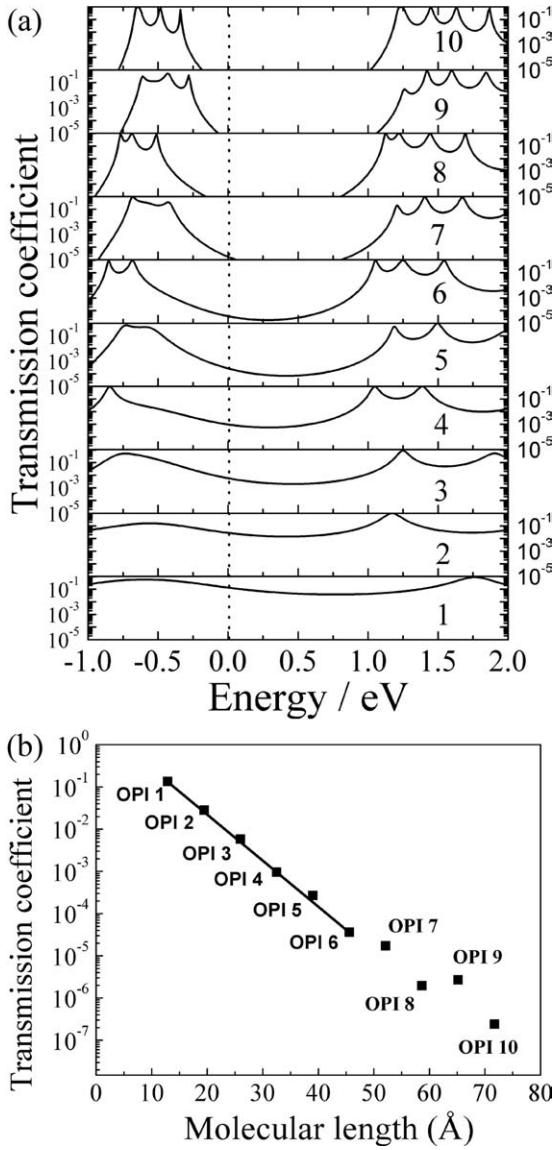

Figure 4. (a) Semilog plots of transmission spectra for the OPI series at zero bias. The dotted line denotes the Fermi level E_F = 0. (b) Semilog plot of transmission coefficient versus length for the OPI series at Femi level E_F = 0. The solid line is linear fit of OPI 1–6.

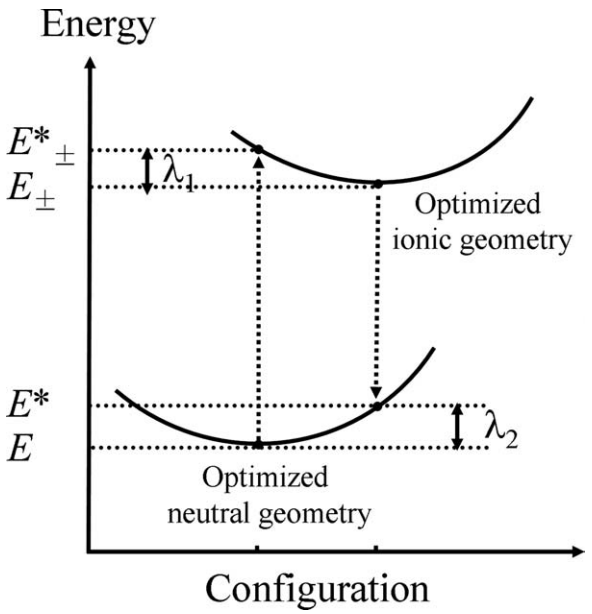

Figure 5. Representation of the reorganization energy involved in the charge transfer process. The two curves represent the potential energies of neutral and ionic molecules. λ_1 and λ_2 show the reorganization energies of two processes involving the removal and addition of a charge, respectively. E and E^* denote the neutral molecule in optimized neutral and ionic geometries, respectively; $E^*_\pm$ and $E_\pm$ are the energies corresponding to the neutral and ionic geometries of the oxidized (or reduced) molecule.

experiments indicates that the hopping current might be involved in the total current, and it becomes more significant with increasing the length. In addition, the intersection and the lower β value after the intersection also suggest that the hopping mechanism becomes dominant in whole transport process. From the comparison, we can conclude that the theoretical simulation with the only mechanism cannot accurately predict the whole transport process, especially, as molecular lengths up to 50 Å.

Besides the molecular length, is there any other indicator of the mechanism transition? We have checked the energy levels of Frontier molecular orbitals (Figure 3b), because they have strong correlation with the conduction behavior. The energy level of the highest occupied molecular orbital (HOMO) is closer to the electrode Fermi level ($E_F = 0$) than the lowest unoccupied molecular orbital (LUMO). For one thing, the energy offsets (E_F–E_{HOMO}) are reduced dramatically from 0.74 (OPI 1) to 0.28 eV (OPI 9) with increasing the repeat unit. The smaller energy offset infers that the removal of an electron from the HOMO is more feasible. For another, the LUMO also shifts toward the Fermi energy for long molecules, indicating an easy hop of the electron from the electrode to the LUMO. Therefore, the thermal emission under ambient conditions (300 K is equal 0.026) may help the electron jumping from molecule to electrode, facilitating the hopping mechanism.

On the other hand, the transmission coefficient curve (Figure 4a) reflects the dynamic feature of the transport system when compared with the static feature of molecular energy levels. Here, the energy is relative to the Fermi level of Au electrodes that is fixed as $E_F = 0$. The first peak below or above the Fermi level primarily originates from the HOMO or LUMO state, respectively. It is clearly shown that the HOMO and LUMO resonances approach the Fermi level as molecular length increases, corresponding to the shift of the molecular orbital energy level. Furthermore, the transmission coefficient of OPI 1 at $E_F = 0$ is 0.13, showing a high efficiency of electron transport for short molecules. As the repeat unit increases to 6, the transmission coefficient decays rapidly to 3.6×10^{-5} for OPI 6. However, the transmission coefficient is less than 10^{-5} for OPI 7–10. Such a low probability of the electron transfer also indicates that the tunneling mechanism is impeded by the energy barrier. In the contrast, hopping conduction is more feasible for those long molecules. More importantly, the transmission coefficient at $E_F = 0$ for OPI 1–6 decreases exponentially with distance as plotted in Figure 4b. As molecular length increases to 50 Å, the low transmission coefficient and non-exponential dependence also reveal the change of electron transport mechanism.

As the hopping involves a series of steps including electron injection to the molecular bridge and transfers between π-conjugated units of the wire, the mechanism of the elementary hopping step can be analogous to a charge transfer reaction, in which an electron or hole is exchanged between two neighboring units, one being in the neutral state and the other being in the ionic state.[32] Thus, the molecule must rearrange as a charge transports along the wire via a series of hops. As demonstrated by Lambert et al.[16] and Sakanoue et al.,[39] reorganization energy λ is an important factor that governs the mobility of charge carriers in molecular wires consisting of π-conjugated units connected by σ-bonded organic spacers, so we evaluated the

Table 2. Reorganization Energies of the OPI Molecules, which Were Calculated at the UDFT Level with the B3LYP Functional and the 6-31G* Basis Set.

Reorganization energy (eV)		OPI 1	OPI 2	OPI 3	OPI 4	OPI 5	OPI 6	OPI 7	OPI 8	OPI 9	OPI 10
Hole transfer	λ_1	0.279	0.148	0.162	0.124	0.111	0.097	0.078	0.070	0.061	0.057
	λ_2	0.711	0.150	0.192	0.151	0.124	0.103	0.133	0.081	0.060	0.063
	λ_+	0.991	0.298	0.355	0.275	0.235	0.201	0.212	0.150	0.122	0.120
Electron transfer	λ_1	0.282	0.229	0.237	0.200	0.183	0.149	0.135	0.112	0.105	0.092
	λ_2	0.238	0.214	0.213	0.200	0.186	0.159	0.166	0.167	0.117	0.100
	λ_-	0.520	0.443	0.450	0.400	0.369	0.308	0.301	0.278	0.222	0.192

λ_1 and λ_2 are obtained from eq 3.

reorganization energy of OPI molecules to gain more insight into the electron transport mechanism.

For each molecule, we obtain a set of four energy values, corresponding to the neutral molecule at the optimized neutral geometry (E), the neutral molecule at the ionic geometry (E^*), the ion at the neutral geometry ($E^*_\pm$), and the ion at the optimized ionic geometry ($E_\pm$). We calculated both the hole and electron transfer, corresponding to the oxidized (λ_+) or reduced (λ_-) states. As shown in Figure 5, these two processes are characterized by reorganization energies λ_1 (the ionization process of the neutral OPI) and λ_2 (the electron or hole attaching process of the OPI ion), respectively. The total reorganization energy λ_+ (λ_-) in the hole (or electron) transfer reaction is a sum of λ_1 and λ_2 by definition[32,39–41]

$$\lambda_\pm = \lambda_1 + \lambda_2 = (E^*_\pm - E_\pm) + (E^* - E) \quad (3)$$

According to optimization results, the ionic structure exhibits a much smaller torsion angle than that of the neutral state with the exception of the cationic OPI 1, which has a dihedral angle of 90°. Especially, the absolute values of torsion angle θ of short OPI molecules, which are in the region of 10–20°, reduce dramatically. In comparison with long molecules, the ionic structure of short OPI molecules shifts toward planarity. The larger geometry differences between the primary and ionic forms for short molecules can yield much higher values of reorganization energy. Table 2 lists the λ values of the OPI series for hole and electron transfer, from which we can observe two important features. First, besides OPI 1, the reorganization energy λ_+ for hole transfer process is lower than λ_- involved in electron transfer process at the same length, indicating the hole transfer plays a key role in the OPI molecules. Second, both λ_+ and λ_- are generally reduced with increasing molecular length barring some fluctuations, in agreement with the evolution of torsion angle. For the hole transfer process, the λ_+ is reduced from 0.991 eV for OPI 1 to 0.120 eV for OPI 10. The low reorganization energy for long molecules suggests that hole hopping is more favorable. As a consequence, the distance dependence of the electron transfer rate for incoherent multistep hopping turns out to be distinct from the exponential law [eq. (1)]. Unlike the single-step coherent tunneling, the elastic scattering cannot properly deal with the incoherent multistep hopping.

Conclusions

Both tunneling and hopping components may contribute to the total current in the molecular junction. The dominant mechanism may gradually change from tunneling to hopping as the molecular length increases. In the theoretical simulation, the elastic scattering theory can satisfactorily predict the tunneling component of the current, so the calculated results are reliable in the short length region. However, when hopping becomes predominant, the calculations by the same method deviate from the experimental measurements. Furthermore, we also found that the type of electron transport mechanism depends on the molecular energy level and reorganization energy. The low reorganization energy for long OPI molecules also indicates that the hopping mechanism is preferred. The present results might be instructive for selecting a proper theoretical method in the simulation of molecular junction.

References

1. McCreery, R. L. Chem Mater 2004, 16, 4477.
2. Li, C.; Pobelov, I.; Wandlowski, T.; Bagrets, A.; Arnold, A.; Evers, F. J Am Chem Soc 2008, 130, 318.
3. Binnig, G.; Quate, C. F.; Gerber, C. Phys Rev Lett 1986, 56, 930.
4. Binnig, G.; Rohrer, H. Helv Phys Acta 1982, 55, 726.
5. Xu, B. Q.; Tao, N. J. Science 2003, 301, 1221.
6. Engelkes, V. B.; Beebe, J. M.; Frisbie, C. D. J Am Chem Soc 2004, 126, 14287.
7. McCreery, R. L. ChemPhysChem 2009, 10, 2387.
8. Nijhuis, C. A.; Reus, W. F.; Barber, J. R.; Dickey, M. D.; Whitesides, G. M. Nano Lett 2010, 10, 3611.
9. Simmons, J. G. J Appl phys 1963, 34, 1793.
10. Sedghi, G.; Sawada, K.; Esdaile, L. J.; Hoffmann, M.; Anderson, H. L.; Bethell, D.; Haiss, W.; Higgins, S. J.; Nichols, R. J. J Am Chem Soc 2008, 130, 8582.
11. Choi, S. H.; Kim, B.; Frisbie, C. D. Science 2008, 320, 1482.
12. Choi, S. H.; Risko, C.; Delgado, M. C. R.; Kim, B.; Bredas, J. L.; Frisbie, C. D. J Am Chem Soc 2010, 132, 4358.
13. Choi, S. H.; Frisbie, C. D. J Am Chem Soc 2010, 132, 16191.
14. Lu, Q.; Liu, K.; Zhang, H. M.; Du, Z. B.; Wang, X. H.; Wang, F. S. ACS Nano 2009, 3, 3861.
15. Hines, T.; Diez-Perez, I.; Hihath, J.; Liu, H.; Wang, Z.-S.; Zhao, J.; Zhou, G.; Mllen, K.; Tao, N. J Am Chem Soc 2010, 132, 11658.
16. Lambert, C.; Noll, G. S. J Nat Mater 2002, 1, 69.
17. Datta, S. Electronic Transport in Mesoscopic Systems; Cambridge University Press: New York, 1997.
18. Stokbro, K.; Taylor, J.; Brandbyge, M. J Am Chem Soc 2003, 125, 3674.
19. Zhang, Y. H.; Chen, Y. B.; Zhou, K. G.; Liu, C. H.; Zeng, J.; Zhang, H. L.; Peng, Y. Nanotechnology 2009, 20, 185504.
20. Kaun, C. C.; Larade, B.; Guo, H. Phys Rev B 2003, 67, 121411.
21. Kaun, C. C.; Guo, H. Nano Lett 2003, 3, 1521.
22. Liu, H. M.; Wang, N.; Zhao, J. W.; Guo, Y.; Yin, X.; Boey, F.; Zhang, H. ChemPhysChem 2008, 9, 1416.
23. Liu, H. M.; Yu, C.; Gao, N.; Zhao, J. ChemPhysChem 2010, 11, 1895.
24. Atomistix Toolkit version 2.0, QuantumWise A/S; Available at:www.quantumwise.com. Accessed on 2006.
25. Brandbyge, M.; Mozos, J.-L.; Ordejón, P.; Taylor, J.; Stokbro, K. Phys Rev B 2002, 65, 165401.
26. Soler, J. M.; Artacho, E.; Gale, J. D.; García, A.; Junquera, J.; Ordejón, P.; Sánchez-Portal, D. J Phys Condens Matter 2002, 14, 2745.
27. Taylor, J.; Guo, H.; Wang, J. Phys Rev B 2001, 63, 245407.
28. See Atomistic Toolkit manual for details:http://www.qutantumwise.com. Accessed on 2006.
29. Stokbro, K.; Taylor, J.; Brandbyge, M. J Am Chem Soc 2003, 125, 3674.
30. Staykov, A.; Nozaki, D.; Yoshizawa, K. J Phys Chem C 2007, 111, 11699.
31. Meir, Y.; Wingreen, N. S. Phys Rev Lett 1992, 68, 2512.
32. Berlin, Y. A.; Hutchison, G. R.; Rempala, P.; Ratner, M. A.; Michl, J. J Phys Chem A 2003, 107, 3970.
33. Frisch, M. J.; Trucks, G. W.; Schlegel, H. B.; Scuseria, G. E.; Robb, M. A.; Cheeseman, J. R.; Montgomery, J. A.; Vreven, T., Jr.; Kudin, K. N.; Burant, J. C.; Millam, J. M.; Iyengar, S. S.; Tomasi, J.; Barone, V.; Mennucci, B.; Cossi, M.; Scalmani, G.; Rega, N.; Petersson,

G. A.; Nakatsuji, H.; Hada, M.; Ehara, M.; Toyota, K.; Fukuda, R.; Hasegawa, J.; Ishida, M.; Nakajima, T.; Honda, Y.; Kitao, O.; Nakai, H.; Klene, M.; Li, X.; Knox, J. E.; Hratchian, H. P.; Cross, J. B.; Adamo, C.; Jaramillo, J.; Gomperts, R.; Stratmann, R. E.; Yazyev, O.; Austin, A. J.; Cammi, R.; Pomelli, C.; Ochterski, J. W.; Ayala, P. Y.; Morokuma, K.; Voth, G. A.; Salvador, P.; Dannenberg, J. J.; Zakrzewski, V. G.; Dapprich, S.; Daniels, A. D.; Strain, M. C.; Farkas, O.; Malick, D. K.; Rabuck, A. D.; Raghavachari, K.; Foresman, J. B.; Ortiz, J. V.; Cui, Q.; Baboul, A. G.; Clifford, S.; Cioslowski, J.; Stefanov, B. B.; Liu, G.; Liashenko, A.; Piskorz, P.; Komaromi, I.; Martin, R. L.; Fox, D. J.; Keith, T.; Al-Laham, M. A.; Peng, C. Y.; Nanayakkara, A.; Challacombe, M.; Gill, P. M. W.; Johnson, B.; Chen, W.; Wong, M. W.; Gonzalez, C.; Pople, J. A. Gaussian 03, Revision C. 02, Gaussian, Inc.: Wallingford CT, 2004.

34. Venkataraman, L.; Klare, J. E.; Nuckolls, C.; Hybertsen, M. S.; Steigerwald, M. L. Nature 2006, 442, 904.
35. Kamenetska, M.; Quek, S. Y.; Whalley, A. C.; Steigerwald, M. L.; Choi, H. J.; Louie, S. G.; Nuckolls, C.; Hybertsen, M. S.; Neaton, J. B.; Venkataraman, L. J Am Chem Soc 2010, 132, 6817.
36. Evers, F.; Weigend, F.; Koentopp, M. Phys Rev B 2004, 69, 235411.
37. Li, Z.; Kosov, D. S. Phys Rev B 2007, 76, 035415.
38. Venkataraman, L.; Klare, J. E.; Tam, I. W.; Nuckolls, C.; Hybertsen, M. S.; Steigerwald, M. L. Nano Lett 2006, 6, 458.
39. Sakanoue, K.; Motoda, M.; Sugimoto, M.; Sakaki, S. J Phys Chem A 1999, 103, 5551.
40. Olofsson, J.; Larsson, S. J Phys Chem B 2001, 105, 10398.
41. Malagoli, M.; Brédas, J. L. Chem Phys Lett 2000, 327, 13.